

Interference Effects in SFVS of Thin Polymer Films: an Experimental and Modeling Investigation

Sarah J. McGall and Paul B. Davies, David J. Neivandt

J. Phys. Chem. B **2004**, *108*, 16030-16039

Zaure

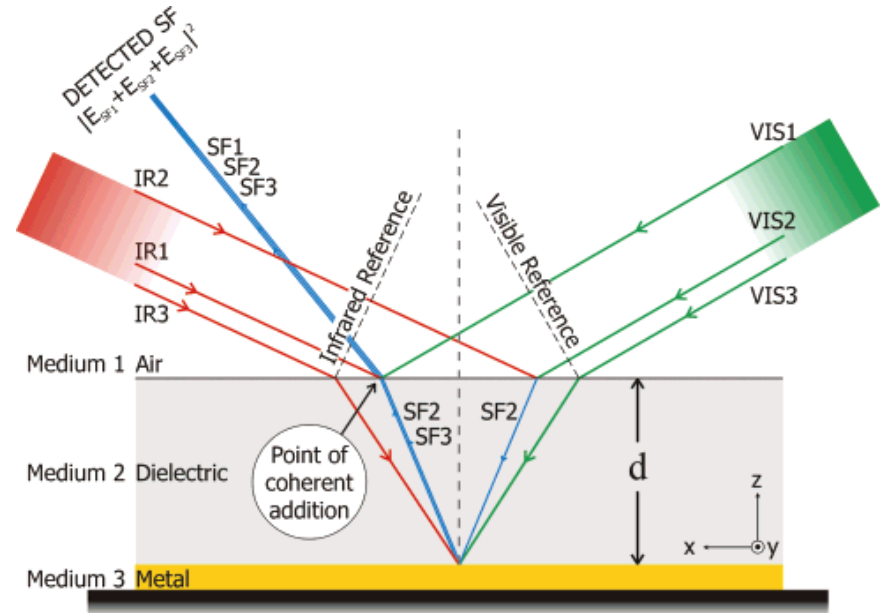
2013.07.19

Outline

- **The Composite Substrate Model**
- **CDC and PDMS films on gold substrates**
- **Model Including Multiple Reflections**
- **Multiple Reflections and a Resonant Contribution from the Polymer/Gold Interface**
- **SFVS of spin-coated CDC and PDMS of different film thicknesses on a gold substrate**
- **SF spectra of PDMS and CDC solvent cast onto gold**

The Composite Substrate Model

SF spectra of a composite substrate consisting of a silane monolayer on mica backed with gold



Schematic diagram of the composite dielectric/metal substrate. The three sum frequency beams generated in the point of coherent addition.

Model Including Multiple Reflections

$$\begin{aligned}\mathbf{E}_z &= (E_z^{\text{I}} + E_z^{\text{R}} + E_z^{\text{M}})\hat{\mathbf{z}} \\ &= (E_z^{\text{I}} + r_{\text{p}}E_z^{\text{I}} + mE_z^{\text{I}})\hat{\mathbf{z}} \\ &= E_{\text{p}}^{\text{I}} \sin\theta_1 (1 + r_{\text{p}} + m)\hat{\mathbf{z}}\end{aligned}$$

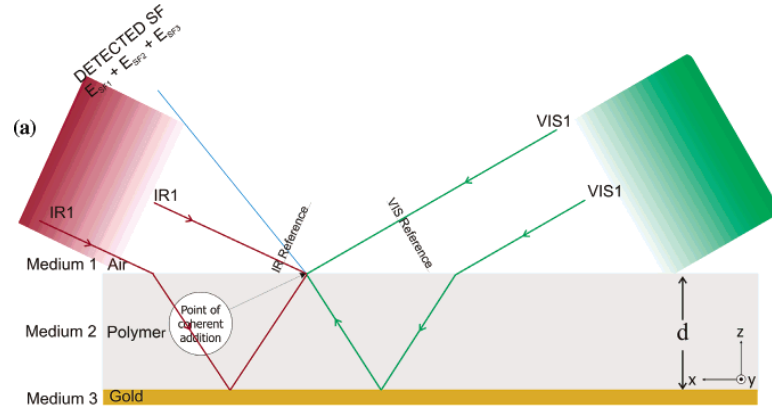
$$\begin{aligned}\mathbf{E}_x &= (E_x^{\text{I}} + E_x^{\text{R}} + E_x^{\text{M}})\hat{\mathbf{x}} \\ &= (E_x^{\text{I}} + r_{\text{p}}E_x^{\text{I}} + mE_x^{\text{I}})\hat{\mathbf{x}} \\ &= E_{\text{p}}^{\text{I}} \cos\theta_1 (1 - r_{\text{p}} - m)\hat{\mathbf{x}}\end{aligned}$$

$$\begin{aligned}m &= t_{12}t_{21}r_{23}\mathrm{e}^{i\alpha_1} + t_{12}t_{21}r_{23}^2r_{21}\mathrm{e}^{i2\alpha_1} + t_{12}t_{21}r_{23}^3r_{21}^2\mathrm{e}^{i3\alpha_1} + \dots \\ &= \frac{t_{12}t_{21}r_{23}\mathrm{e}^{i\alpha_1}}{1 - r_{21}r_{23}\mathrm{e}^{i\alpha_1}}\end{aligned}$$

where α_1 is given by

$$\alpha_1 = \frac{4\pi d}{\lambda} \left(\frac{n_2}{\cos\theta_{23}} - n_1 \tan\theta_{23} \sin\theta_{12} \right)$$

Ray diagram: the generation of the SF1 beam



SF spectra of spin-coated CDC and PDMS films on gold substrates

$$K_{x,vis}^{mod} = \cos\theta_{I,vis}(1 - r_p - m)$$

$$K_{z,vis}^{mod} = \sin\theta_{I,vis}(1 + r_p + m)$$

$$K_{x,IR}^{mod} = -\cos\theta_{I,IR}(1 - r_p + m)$$

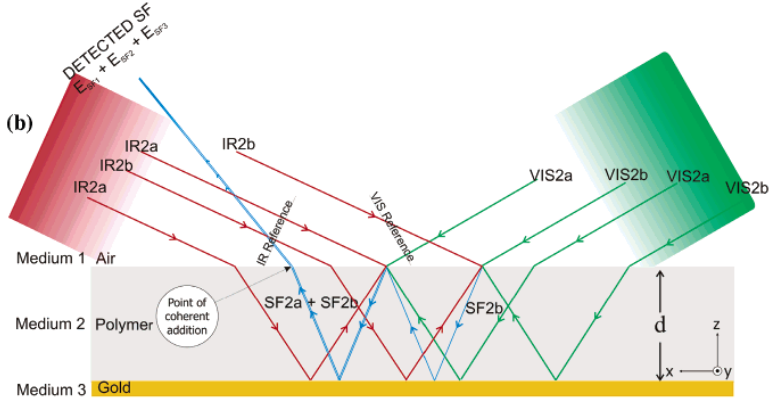
$$K_{z,IR}^{mod} = \sin\theta_{I,IR}(1 + r_p + m)$$

$$\mathbf{E}_{p,SF1} \propto |\mathbf{E}_{x,SF1}| + |\mathbf{E}_{z,SF1}|$$

$$\propto |L_x \mathbf{P}_{x,SF1}^{(2)}| + |L_z \mathbf{P}_{z,SF1}^{(2)}|$$

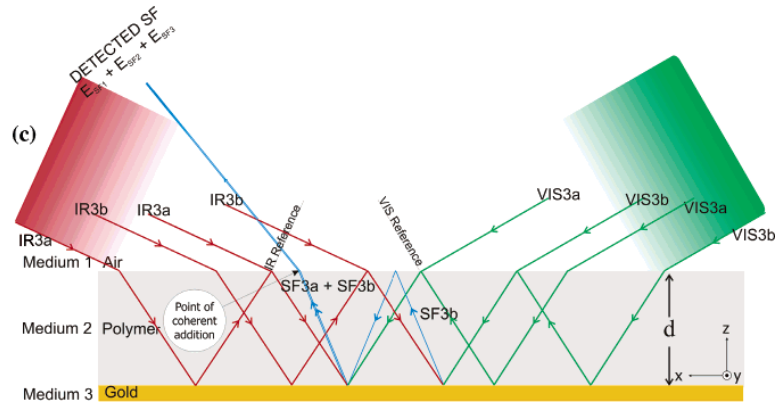
$$\propto |(L_{r,x} \chi_{xxz}^{(2)} K_{x,vis}^{mod} K_{z,IR}^{mod} + L_{r,x} \chi_{xzx}^{(2)} K_{z,vis}^{mod} K_{x,IR}^{mod}) e^{i(\Delta_{vis1} + \Delta_{IR1})}| + |(L_{r,z} \chi_{zzx}^{(2)} K_{z,vis}^{mod} K_{z,IR}^{mod} + L_{r,z} \chi_{zxx}^{(2)} K_{x,vis}^{mod} K_{x,IR}^{mod}) e^{i(\Delta_{vis1} + \Delta_{IR1})}|$$

Ray diagram: the generation of the SF2 beam



$$\begin{aligned}
 \mathbf{E}_{p,\text{SF2}} &\propto |\mathbf{E}_{x,\text{SF2}}| + |\mathbf{E}_{z,\text{SF2}}| \\
 &\propto |L_{t,x} \mathbf{P}_{x,\text{SF2}}^{(2)}| + |L_{t,z} \mathbf{P}_{z,\text{SF2}}^{(2)}| \\
 &\propto |(m_{\text{SF2}} L_{t,x} \chi_{xxz}^{(2)} K_{x,\text{vis}}^{\text{mod}} K_{z,\text{IR}}^{\text{mod}} + \\
 &\quad m_{\text{SF2}} L_{t,x} \chi_{xzx}^{(2)} K_{z,\text{vis}}^{\text{mod}} K_{x,\text{IR}}^{\text{mod}}) e^{i(\Delta_{\text{vis1}} + \Delta_{\text{IR1}})}| + \\
 &\quad |(m_{\text{SF2}} L_{t,z} \chi_{zzz}^{(2)} K_{z,\text{vis}}^{\text{mod}} K_{z,\text{IR}}^{\text{mod}} + \\
 &\quad m_{\text{SF2}} L_{t,z} \chi_{zxx}^{(2)} K_{x,\text{vis}}^{\text{mod}} K_{x,\text{IR}}^{\text{mod}}) e^{i(\Delta_{\text{vis1}} + \Delta_{\text{IR1}})}| \\
 m_{\text{SF2}} &= r_{23} t_{21} e^{i\alpha_2} + r_{23}^2 r_{21} t_{21} e^{i2\alpha_2} + r_{23}^3 r_{21}^2 t_{21} e^{i3\alpha_2} + \dots \\
 &= \frac{r_{23} t_{21} e^{i\alpha_2}}{1 - r_{23} r_{21} e^{i\alpha_2}} \\
 \alpha_2 &= \frac{4\pi n_2 d}{\cos\theta_{23} \lambda}
 \end{aligned}$$

Ray diagram: the generation of the SF3 beam



$$\mathbf{E}_{p,SF3} \propto |L_{r,z} \mathbf{P}_{z,SF3}^{(2)}|$$

$$\propto |m_{SF3} L_{r,z} E_{NR} e^{i(\epsilon + \Delta_{vis3} + \Delta_{IR3})} K_{z,vis}^{gold} K_{z,IR}^{gold}|$$

$$K_{z,vis}^{gold} = \sin \theta_{I,vis} m_{gold} (1 + r_p)$$

$$K_{z,IR}^{gold} = \sin \theta_{I,IR} m_{gold} (1 + r_p)$$

$$m_{gold} = \frac{t_{21}}{1 - r_{23} r_{21} e^{i\alpha_1}}$$

$$m_{SF3} = \frac{t_{21} e^{i\Delta_{SF3}}}{1 - r_{23} r_{21} e^{i\alpha_2}}$$

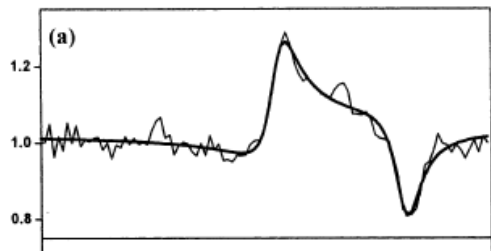
Multiple Reflections and a Resonant Contribution from the Polymer/Gold Interface

$$\begin{aligned}
 \mathbf{E}_{\text{p,SF4}} &\propto |\mathbf{E}_{\text{x,SF4}}| + |\mathbf{E}_{\text{z,SF4}}| \\
 &\propto |L_{r,x} \mathbf{P}_{\text{x,SF4}}^{(2)}| + |L_{r,z} \mathbf{P}_{\text{z,SF4}}^{(2)}| \\
 &\propto |(m_{\text{SF3}} L_{r,x} \chi_{\text{xxz}}^{(2)} K_{\text{x,vis}}^{\text{gold}} K_{\text{z,IR}}^{\text{gold}} + \\
 &\quad m_{\text{SF3}} L_{r,z} \chi_{\text{zzz}}^{(2)} K_{\text{z,vis}}^{\text{gold}} K_{\text{z,IR}}^{\text{gold}}) e^{i(\Delta_{\text{vis3}} + \Delta_{\text{IR3}})}|
 \end{aligned}$$

The total intensity of the generated SF light may consequently be expressed as

$$\begin{aligned}
 I_{\text{p,SF}} = & |\mathbf{E}_{\text{x,SF1}} + \mathbf{E}_{\text{x,SF2}} + \mathbf{E}_{\text{x,SF3}} + \mathbf{E}_{\text{x,SF4}}|^2 + \\
 & |\mathbf{E}_{\text{z,SF1}} + \mathbf{E}_{\text{z,SF2}} + \mathbf{E}_{\text{z,SF3}} + \mathbf{E}_{\text{z,SF4}}|^2
 \end{aligned}$$

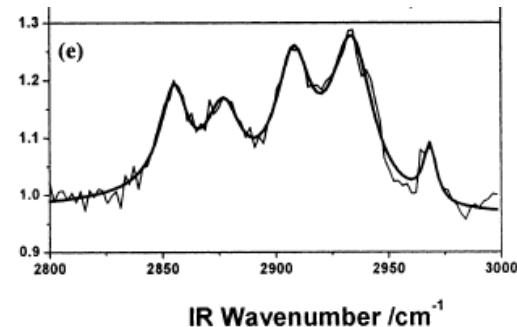
SF spectra of PDMS and CDC solvent cast onto gold



The SF spectrum of PDMS:

the r+ symmetric (2908 cm^{-1})

the r- anti-symmetric (2963 cm^{-1})



The SF spectrum of CDC :

the r+ mode of the PDMS backbone (2908 cm^{-1})

the resonance at 2968 cm^{-1} (a combination of the r- modes of the backbone and the cetyl side chains of the polymer)



The difference in r- phase for the original solvent cast CDC and PDMS spectra is due solely to different film thicknesses in the solvent cast samples.

SFVS of spin-coated CDC and PDMS of different film thicknesses on a gold substrate.

For both PDMS and CDC:

- the 2908 cm^{-1} r+ resonance of the methyl groups is a spectral peak (positive phase) over the thickness range investigated.
- the r- resonance is a spectral peak (positive phase) at small polymer film thicknesses, changes to a differential shape as the film thickness increases, and finally becomes a spectral dip (negative phase) for the thickest samples investigated.

